ANALYTICAL AND NUMERICAL TECHNIQUES FOR SOLVING THE BELOUSOV-ZHABOTINSKII DIFFUSION MODEL
A Chemical Application

by

Khalid K. ALI[a*], Mohamed S. MOHAMED[b], and Mahamed A. SHAALAN[c]

[a] Mathematics Department, Faculty of Science, Al-Azhar University, Cairo, Egypt
[b] Department of Mathematics, College of Science, Taif University, Taif, Saudi Arabia
[c] Higher Technological Institute, Tenth of Ramadan City, Egypt

Original scientific paper
https://doi.org/10.2298/TSCI2406943A

The primary focus of this paper is on finding an analytical solution for the Belousov-Zhabotinskii system. The Belousov-Zhabotinskii reaction is a chemical reaction that exhibits oscillating behavior in the concentrations of its reactants and products. The reaction is named after Boris Belousov and Anatol Zhabotinsky, who discovered it in the 1950. The Belousov-Zhabotinskii reaction was first described by a system of equations in 1983 [1]. It serves as a model for numerous, more complex biological and biochemical processes. In this work, we present the soliton solution for the Belousov-Zhabotinskii system using the (G'/G)-expansion technique. We also study the solutions numerically using the cubic B-spline method. Finally, 2-D and 3-D graphs are used to visualize the obtained soliton solutions.

Key words: *Belousov-Zhabotinskii system, (G'/G)-expansion technique, soliton solutions, cubic B-spline method*

Introduction

The Belousov-Zhabotinskii (BZ) reaction is a type of reaction-diffusion system, which means it involves both chemical reactions and the diffusion of substances through space. The reaction involves a set of chemical species, typically including a metal catalyst, an oxidizing agent, and an organic substrate. When these substances are mixed together in a solution, they undergo a series of reactions that produce a range of intermediate and final products. The oscillating behavior in the BZ reaction arises due to a series of autocatalytic reactions, where the products of one reaction serve as a catalyst for the next reaction. The reaction system can also exhibit spatial patterns, such as the formation of concentric rings or spirals, which are caused by the interaction of chemical reactions and the diffusion of substances through space. The BZ reaction has been extensively studied in the field of non-linear dynamics and serves as a model system for understanding the emergence of complex behavior in non-linear systems. It has also found applications in areas like chemical oscillators, sensors, and even art installations. The BZ reaction is one of several reactions that exhibit similar wave and pattern creation phenomena, which has sparked investigations into their use as paradigms for biological pattern formation systems. These studies have significantly improved our understanding of the intricate wave behavior observed in embryonic development, the heart, and other bodily organs.

* Corresponding author, e-mail: khalidkarem2012@azhar.edu.eg

The main factor determining the speed of the wavefront in these systems is the concentration of certain chemical species, such as the bromide ion (Br^-) and the bromous acid ($HBrO_2$), denoted as v and u, respectively, in a simplified reaction sequence:

$$A + v \rightleftharpoons^{k_1} u + P,\ \ u + v \rightleftharpoons^{k_2} 2P,\ \ A + u \rightleftharpoons^{k_3} 2u,\ \ 2u \rightleftharpoons^{k_4} P + A$$

where the constants k_1, k_2, k_3, and k_4 present the rate, A (BrO^-) the concentration, and P the compound HbrO. By utilizing lowercase letters for concentrations, applying the law of mass action this scheme:

$$u_t = k_1 av - k_2 uv + k_3 a_u - k_4 u^2 + Du_{xx},\ \ v_t = -k_1 av - k_2 uv + Dv_{xx}$$

where D is the coefficient of diffusion. A suitable non-dimensional:

$$\Phi = \frac{k_4 u}{k_3 a},\quad \Psi = \frac{k_2 v}{k_3 ar},\quad x^* = \left(\frac{k_3 a}{D}\right)^{1/2} x,\quad t^* = k_3 at,\ L = \frac{k_1 k_4}{k_2 k_3},\ M = \frac{k_1}{k_3},\ \ b = \frac{k_2}{k_4}$$

where r is the parameter that announce that the concentration of bromide ions far in advance of the wavefront can be changed experimentally. For simplicity omitting the asterisks:

$$\Phi_t = Lr\Psi + \Phi(1 - \Phi - r\Psi) + \Phi_{xx},\ \Psi_t = -M\Psi - b\Phi\Psi + \Psi_{xx}$$

since $L \approx M = O(10^{-4})$, $L \ll 1$, and $M \ll 1$, we can disregard these terms and reach at the following model: The system describes BZ reaction:

$$\Phi_t = \Phi_{xx} + \Phi(1 - \Phi - r\Psi),\ \ \Psi_t = \Psi_{xx} - b\Phi\Psi$$

searching for travelling wavefront solutions, as it lowers the level of the bromide ion, the wave goes from a zone of high bromous acid concentration one of low bromous acid concentration. Thus, we search for waves with boundary conditions:

$$\Phi(-\infty, t) = 0,\ \Psi(-\infty, t) = 1,\ \Phi(\infty, t) = 1,\ \Psi(\infty, t) = 0$$

where the functions Ψ, Φ introduce the bromide ion and bromic acid concentrations, r and b are the positive constants, for more details see [2]. We employ the variable change $\Phi = \Phi$ and $\Psi = 1 - \Psi$ [3], which results:

$$\Phi_t = \Phi_{xx} + \Phi(1 - r - \Phi + r\Psi),\ \ \Psi_t = \Psi_{xx} + b\Phi(1 - \Psi) \tag{1}$$

The existence of traveling wave solutions is studied under different conditions by many authors: Murray [4, 5], Tyson [6], Ye *et al*. [7, 8], Li [9], Li *et al*. [10], Trofimchuk *et al*. [11] study the stability and the uniqueness of monotone wavefronts, Manoranjan *et al*. [12] use the finite element method to obtain the wave solution, four kinds of explicit wave front solutions are presented by Wang *et al*. [13], Quinney [14] present the solution using the finite difference method. Later, Kudryashov *et al.* [15] give solutions related to the Weierstrass elliptic function. There exist various numerical methods [16-24] as the finite difference method, the finite element method, and the basis spline functions method are which also commonly applied to engineering and physical and chemical applications.

Methodology outlines

The (G'/G)-expansion technique

Exhibiting the main steps in the current section illustrate the new form of the (G'/G)-expansion method [25-27]. Presumption the model equation is given:

$$F(\psi, \psi_x, \psi_t, \psi_{xx}, \psi_{tt}, \psi_{xt}) = 0 \tag{2}$$

where F is the polynomial in $\psi = \psi(x,t)$ and its partial derivatives. Inserting the wave transformations:

$$\eta = x + ct, \quad \psi(x,t) = \psi(\eta) \tag{3}$$

where $c > 0$ is the speed of the wave. The eq. (2) switched to the ordinary differential equation:

$$H(\psi, \psi', \psi'', \psi''', \psi'''') = 0 \tag{4}$$

– *Step 1*: Next we present the solution of eq. (4):

$$\Psi(\eta) = \sum_{j=0}^{N} f_j \left(\frac{G'}{G}\right)^j \tag{5}$$

where $G = G(\eta)$ satisfy the ODE:

$$G''(\eta) = -\lambda G'(\eta) - \mu G(\eta) \tag{6}$$

where $f_1(j = 0, 1, 2, ..., N)$, $f_N \neq 0$, λ and μ, are constants.

– *Step 2*: Balancing the highest power non-linear term with the highest order derivative term in (4), to calculate the value of N.

– *Step 3*: Three categories of solutions of eq. (6) are given:

Case 1. The $\lambda^2 - 4\mu > 0$, the solutions are hyperbolic functions:

$$\frac{G'}{G} = \frac{\sqrt{\lambda^2 - 4\mu}}{2} \times \frac{h_1 \sinh\left(\frac{\eta}{2}\sqrt{\lambda^2 - 4\mu}\right) + h_2 \cosh\left(\frac{\eta}{2}\sqrt{\lambda^2 - 4\mu}\right)}{h_1 \cosh\left(\frac{\eta}{2}\sqrt{\lambda^2 - 4\mu}\right) + h_2 \sinh\left(\frac{\eta}{2}\sqrt{\lambda^2 - 4\mu}\right)} - \frac{\lambda}{2} \tag{7}$$

Case 2. The $\lambda^2 - 4\mu < 0$, the solutions are trigonometric functions:

$$\frac{G'}{G} = \frac{\sqrt{4\mu - \lambda^2}}{2} \times \frac{-h_1 \sin\left(\frac{\eta}{2}\sqrt{4\mu - \lambda^2}\right) + h_2 \cos\left(\frac{\eta}{2}\sqrt{4\mu - \lambda^2}\right)}{h_1 \cos\left(\frac{\eta}{2}\sqrt{4\mu - \lambda^2}\right) + h_2 \sin\left(\frac{\eta}{2}\sqrt{4\mu - \lambda^2}\right)} - \frac{\lambda}{2} \tag{8}$$

Case 3. The $\lambda^2 - 4\mu = 0$, the solutions are rational functions:

$$\frac{G'}{G} = \frac{h_2}{h_1 + h_2\eta} - \frac{\lambda}{2} \tag{9}$$

– *Step 4*: Inserting eqs. (5) and (6) into eq. (4), use Mathematica program to solve the system yields when setting the coefficients with the same power of (G'/G) equal to zero.

Applications

Employing the wave transformation (3) on (1), we get the next ODE system of equations:

$$\begin{gathered} \Phi(\eta)(-1 + r + \Phi(\eta) - r\Psi(\eta)) + c\Phi'(\eta) - \Phi''(\eta) = 0 \\ b\Phi(\eta)(-1 + \Psi(\eta)) + c\Psi'(\eta) - \Psi''(\eta) = 0 \end{gathered} \tag{10}$$

Determine the values of M and N from eq. (10):

– the $\Phi(\eta)\Psi(\eta)$ with $\Phi'' \Rightarrow M = 2$ and
– the $\Phi(\eta)\Psi(\eta)$ with $\Psi'' \Rightarrow (\eta) \Rightarrow N = 2$.

Results employing the G'/G-expansion technique

Based upon eq. (5), the solution of eq. (10) is stated next:

$$\Phi(\eta) = f_0 + f_1\left(\frac{G'(\eta)}{G(\eta)}\right) + f_2\left(\frac{G'(\eta)}{G(\eta)}\right)^2,\ \Psi(\eta) = m_0 + m_1\left(\frac{G'(\eta)}{G(\eta)}\right) + m_2\left(\frac{G'(\eta)}{G(\eta)}\right)^2 \tag{11}$$

We arrive at the following system by inserting eq. (11) into eq. (10) and setting the coefficients with equal powers of $G(\eta)$ to zero:

$$\begin{gathered}
\mu(-f_1(c+\lambda) - 2\mu f_2) + f_0(r - 1 + f_0 - rm_0) = 0 \\
2\mu f_2(c+3\lambda) + f_1(1 - r + \lambda(c+\lambda) + 2\mu - 2f_0 + rm_0) + rf_0m_1 = 0 \\
-f_1^2 + f_2(1 - r + 2\lambda(c+2\lambda) + 8\mu - 2f_0 + rm_0) + f_1(c + 3\lambda + rm_1) + rf_0m_2 = 0 \\
f_2(2c + 10\lambda + rm_1) + f_1(2 - 2f_2 + rm_2) = 0 \\
f_2(-6 + f_2 - rm_2) = 0 \\
-bf_0 + bf_0m_0 - c\mu m_1 - \lambda\mu m_1 - 2\mu^2 m_2 = 0 \\
bf_1(m_0 - 1) - m_1(c\lambda + \lambda^2 + 2\mu - bf_0) - 2\mu m_2(c + 3\lambda) = 0 \\
bf_2(m_0 - 1) - m_1(c + 3\lambda - bf_1) + (-2c\lambda - 4\lambda^2 - 8\mu + bf_0)m_2 = 0 \\
m_1(bf_2 - 2) + m_2(-2c - 10\lambda + bf_1) = 0 \\
(-6 + bf_2)m_2 = 0
\end{gathered} \tag{12}$$

When the former system of equations is solved, two sets of solutions are obtained:

– Set 1

$$\begin{gathered}
f_0 = 2\mu,\ f_1 = 2\lambda,\ f_2 = 2,\quad m_0 = -\frac{1}{r^2}\left(r - r^2 + r\lambda^2 + \lambda\sqrt{r^2(3 + \lambda^2 - 4\mu)}\right) \\
m_1 = -\frac{4r\lambda + 2\sqrt{r^2(3 + \lambda^2 - 4\mu)}}{r^2},\quad m_2 = -\frac{4}{r},\ c = \frac{1}{r}\sqrt{r^2(3 + \lambda^2 - 4\mu)},\ b = 3
\end{gathered} \tag{13}$$

– Set 2

$$\begin{gathered}
f_0 = \frac{\lambda^4 + \lambda\sqrt{(\lambda^2 - 4\mu)^3} - 6\mu\lambda^2 + 8\mu^2}{2(\lambda^2 - 4\mu)^2},\ f_1 = \frac{\lambda^3 - 4\lambda\mu + \sqrt{(\lambda^2 - 4\mu)^3}}{(\lambda^2 - 4\mu)^2},\ f_2 = \frac{1}{\lambda^2 - 4\mu} \\
m_0 = \frac{1}{2r(\lambda^2 - 4\mu)^2}(6\lambda^6 + \lambda^4(-1 + 2r - 84\mu) - 6\lambda^3\sqrt{(\lambda^2 - 4\mu)^3} + \lambda(1 + 24\mu)\sqrt{(\lambda^2 - 4\mu)^3} + \\
+8\mu^2(-3 + 4r - 72\mu) + 2\mu\lambda^2(5 - 8r + 192\mu)) \\
m_1 = -\frac{(-1 + 6\lambda^2 - 24\mu)(\lambda^3 - 4\lambda\mu + \sqrt{(\lambda^2 - 4\mu)^3})}{r(\lambda^2 - 4\mu)^2},\ m_2 = \frac{1 - 6\lambda^2 + 24\mu}{r\lambda^2 - 4r\mu} \\
c = \frac{5\sqrt{(\lambda^2 - 4\mu)^3}}{\lambda^2 - 4\mu},\ b = 6(\lambda^2 - 4\mu)
\end{gathered} \tag{14}$$

Next we present the three classes of soliton solutions:

Case 1. The $\lambda^2 - 4\mu > 0$, the solutions are hyperbolic functions:

$$\Phi(x,t) = f_0 + f_1\left(\frac{\sqrt{\lambda^2-4\mu}}{2}\times\frac{h_1\sinh(\frac{1}{2}(x+ct)\sqrt{\lambda^2-4\mu})+h_2\cosh\left(\frac{1}{2}(x+ct)\sqrt{\lambda^2-4\mu}\right)}{h_1\cosh\left(\frac{1}{2}(x+ct)\sqrt{\lambda^2-4\mu}\right)+h_2\sinh\left(\frac{1}{2}(x+ct)\sqrt{\lambda^2-4\mu}\right)}-\frac{\lambda}{2}\right)+$$
$$+f_2\left(\frac{\sqrt{\lambda^2-4\mu}}{2}\times\frac{h_1\sinh\left(\frac{1}{2}(x+ct)\sqrt{\lambda^2-4\mu}\right)+h_2\cosh\left(\frac{1}{2}(x+ct)\sqrt{\lambda^2-4\mu}\right)}{h_1\cosh\left(\frac{1}{2}(x+ct)\sqrt{\lambda^2-4\mu}\right)+h_2\sinh\left(\frac{1}{2}(x+ct)\sqrt{\lambda^2-4\mu}\right)}-\frac{\lambda}{2}\right)^2$$
$$\Psi(x,t) = m_0 + m_1\left(\frac{\sqrt{\lambda^2-4\mu}}{2}\times\frac{h_1\sinh\left(\frac{1}{2}(x+ct)\sqrt{\lambda^2-4\mu}\right)+h_2\cosh\left(\frac{1}{2}(x+ct)\sqrt{\lambda^2-4\mu}\right)}{h_1\cosh\left(\frac{1}{2}(x+ct)\sqrt{\lambda^2-4\mu}\right)+h_2\sinh\left(\frac{1}{2}(x+ct)\sqrt{\lambda^2-4\mu}\right)}-\frac{\lambda}{2}\right)+ \quad (15)$$
$$+m_2\left(\frac{\sqrt{\lambda^2-4\mu}}{2}\times\frac{h_1\sinh\left(\frac{1}{2}(x+ct)\sqrt{\lambda^2-4\mu}\right)+h_2\cosh\left(\frac{1}{2}(x+ct)\sqrt{\lambda^2-4\mu}\right)}{h_1\cosh\left(\frac{1}{2}(x+ct)\sqrt{\lambda^2-4\mu}\right)+h_2\sinh\left(\frac{1}{2}(x+ct)\sqrt{\lambda^2-4\mu}\right)}-\frac{\lambda}{2}\right)^2$$

Case 2: The $\lambda^2 - 4\mu < 0$, the solutions are trigonometric functions:

$$\Phi(x,t) = f_0 + f\left(\frac{\sqrt{4\mu-\lambda^2}}{2}\times\frac{-h_1\sin\left(\frac{1}{2}(x+ct)\sqrt{4\mu-\lambda^2}\right)+h_2\cos\left(\frac{1}{2}(x+ct)\sqrt{4\mu-\lambda^2}\right)}{h_1\cos\left(\frac{1}{2}(x+ct)\sqrt{4\mu-\lambda^2}\right)+h_2\sin\left(\frac{1}{2}(x+ct)\sqrt{4\mu-\lambda^2}\right)}-\frac{\lambda}{2}\right)+$$
$$+f_2\left(\frac{\sqrt{4\mu-\lambda^2}}{2}\times\frac{-h_1\sin\left(\frac{1}{2}(x+ct)\sqrt{4\mu-\lambda^2}\right)+h_2\cos\left(\frac{1}{2}(x+ct)\sqrt{4\mu-\lambda^2}\right)}{h_1\cos\left(\frac{1}{2}(x+ct)\sqrt{4\mu-\lambda^2}\right)+h_2\sin\left(\frac{1}{2}(x+ct)\sqrt{4\mu-\lambda^2}\right)}-\frac{\lambda}{2}\right)^2$$
$$\Psi(x,t) = m_0 + m_1\left(\frac{\sqrt{4\mu-\lambda^2}}{2}\times\frac{-h_1\sin\left(\frac{1}{2}(x+ct)\sqrt{4\mu-\lambda^2}\right)+h_2\cos\left(\frac{1}{2}(x+ct)\sqrt{4\mu-\lambda^2}\right)}{h_1\cos\left(\frac{1}{2}(x+ct)\sqrt{4\mu-\lambda^2}\right)+h_2\sin\left(\frac{1}{2}(x+ct)\sqrt{4\mu-\lambda^2}\right)}-\frac{\lambda}{2}\right)+ \quad (16)$$
$$+m_2\left(\frac{\sqrt{4\mu-\lambda^2}}{2}\times\frac{-h_1\sin\left(\frac{1}{2}(x+ct)\sqrt{4\mu-\lambda^2}\right)+h_2\cos\left[\frac{1}{2}(x+ct)\sqrt{4\mu-\lambda^2}\right]}{h_1\cos\left(\frac{1}{2}(x+ct)\sqrt{4\mu-\lambda^2}\right)+h_2\sin\left(\frac{1}{2}(x+ct)\sqrt{4\mu-\lambda^2}\right)}-\frac{\lambda}{2}\right)^2$$

Case 3: The $\lambda^2 - 4\mu = 0$, the solutions are rational functions:

$$\Phi(x,t) = f_0 + f_1\left(\frac{h_2}{h_1+h_2(x+ct)}-\frac{\lambda}{2}\right)+f_2\left(\frac{h_2}{h_1+h_2(x+ct)}-\frac{\lambda}{2}\right)^2$$
$$\Psi(x,t) = m_0 + m_1\left(\frac{h_2}{h_1+h_2(x+ct)}-\frac{\lambda}{2}\right)+m_2\left(\frac{h_2}{h_1+h_2(x+ct)}-\frac{\lambda}{2}\right)^2 \quad (17)$$

Graphical illustrations and discussion

A graph is a way to show data in a visual way to illustrate solutions, some of our solutions are presented in two and three dimensions. In fig. 1, we show the graphs of eq. (15) with Set 1 eq. (13) applying the (G'/G) method at $r = 0.3$, $\mu = 0.0001$, $\lambda = 0.4$, $h_1 = 0.8$, and $h_2 = 0.1$. With passing time, we observe the wave shifting to the left. The wave has a bell-like soliton and is moving to the left. In fig. 2, we present the graphs of eq. (16) with Set 1 eq. (13) employing the (G'/G) method at $r = 1.01$, $\mu = 0.001$, $\lambda = 0.01$, $h_1 = 0.5$, and $h_2 = 0.1$. Both graphs show the wave is flipped and is moving to the left. Lastly, fig. 3 show the graphs of Φ and Ψ of eq. (15) with Set 2 eq. (14) employing the (G'/G) method at $r = 0.8$, $\mu = 0.001$, $h_1 = 0.3$, and $h_2 = 0.1$ and $b = 0.91$, $b = 1.16$, and $b = 1.44$. We exhibit the variation in Φ and Ψ as the values of the paramerter b, which can be summarized.

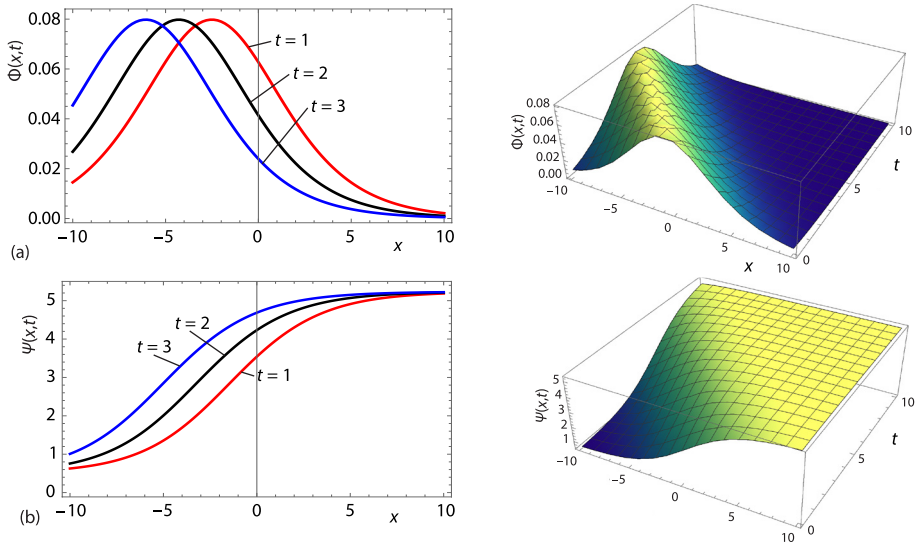

Figure 1. The Φ (a) and Ψ (b), eq. (15) with Set 1 eq. (13) employing the (G'/G) method at $r = 0.3$, $\mu = 0.0001$, $\lambda = 0.4$, $h_1 = 0.8$, and $h_2 = 0.1$

Parameter b: this parameter determines the strength of the feedback loop between the two variables, Φ and Ψ. When b is small, the feedback loop is weak, and the concentration of Ψ has little effect on the dynamics of the system. As b increases, the feedback loop becomes stronger, and the oscillations in the system become more pronounced. Moreover, when b is very large, the system may exhibit chaotic behavior.

Numerical illustrations

We utilize the cubic B-spline collocation method to find the numerical solutions of the BZ eq. (1) in the following procedures:

– *Procedure 1*. We use the following initial and boundary conditions to solve BZ eq. (1):

$$\Phi(x,0) = \mathbf{f}_1(x),\ \ \Psi(x,0) = \mathbf{f}_2(x),\ \ \mathbf{a} \le x \le \mathbf{b}$$
$$\Phi(\mathbf{a},t) = \mathbf{f}_3(t),\ \ \Phi(\mathbf{b},t) = \mathbf{f}_4(t),\ \ \Psi(\mathbf{a},t) = \mathbf{f}_5(t),\ \ \Psi(\mathbf{b},t) = \mathbf{f}_6(t) \tag{18}$$

– *Procedure 2*. We suppose $x \in [\mathbf{a}, \mathbf{b}]$ is split into $\mathbf{N}$ equal sub-intervals with step length

$$\mathbf{h} = \frac{\mathbf{b}-\mathbf{a}}{\mathbf{n}} = x_{\mathbf{i}+1} - x_{\mathbf{i}} \quad \text{for} \quad \mathbf{i} = 0,1,...,\mathbf{n}$$

and let the time levels with $\Delta t > 0$ is $t_{\mathbf{j}} = \mathbf{j}\Delta t$ for $\mathbf{j} = 0.\ 1,\ ...,\ \mathbf{m}$, where $\mathbf{m}$ is the integer.

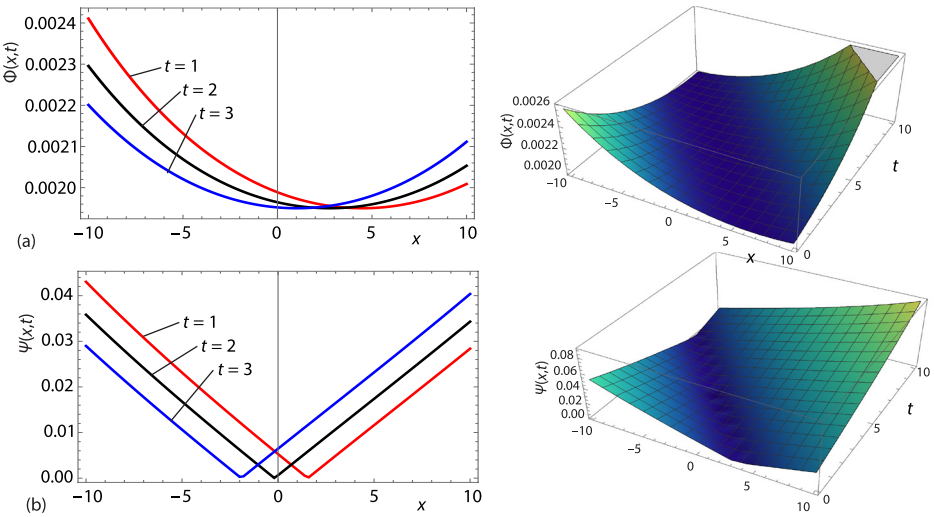

Figure 2. The Φ (a) and Ψ (b), eq. (16) with Set 1 eq. (13) employing the (G'/G) method at $r = 01.01$, $\mu = 0.001$, $\lambda = 0.01$, $h_1 = 0.5$, and $h_2 = 0.1$

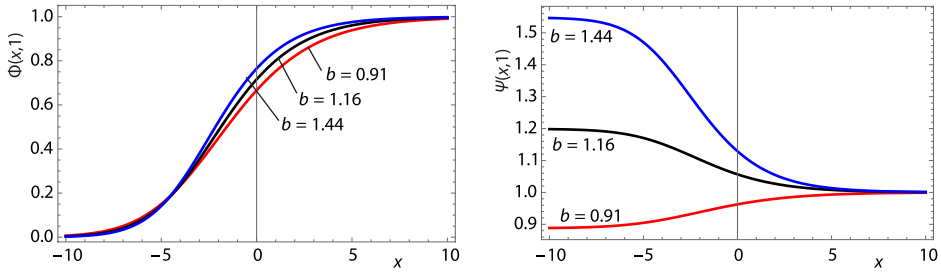

Figure 3. The graphs of Φ and Ψ of eq. (15) with Set 2 eq. (14) employing the (G'/G) method at $r = 0.8$, $\mu = 0.001$, $h_1 = 0.3$, and $h_2 = 0.1$ and $b = 0.91$, $b = 1.16$, and $b = 1.44$

– *Procedure 3*. To obtain the numerical solutions of the BZ eq. (1) $\tilde{\Phi}(x, t)$ and $\tilde{\Psi}(x, t)$ that are equivalent to the exact solutions $\Phi(x, t)$ and $\Psi(x, t)$:

$$\tilde{\Phi}(x,t) = \sum_{\mathbf{i}=-1}^{\mathbf{n}+1} \phi_{\mathbf{i}}(x)\varrho_{\mathbf{i}}(t), \quad \tilde{\Psi}(x,t) = \sum_{\mathbf{i}=-1}^{\mathbf{n}+1} \psi_{\mathbf{i}}(x)\upsilon_{\mathbf{i}}(t) \tag{19}$$

where $\phi_{\mathbf{i}}(x)$ and $\psi_{\mathbf{i}}(x)$ are the cubic B-spline functions, ($\mathbf{i} = -1, 0, ..., \mathbf{n} + 1$), at the nodal points $x_{\mathbf{i}}$ are depicted on the interval [**a**, **b**] by [16]:

$$\phi_{\mathbf{i}}(x) = \psi_{\mathbf{i}}(x) = \frac{1}{\mathbf{h}^3}\begin{cases} (x - x_{\mathbf{i}-2})^3 & x_{\mathbf{i}-2} \le x \le x_{\mathbf{i}-1} \\ \mathbf{h}^3 + 3\mathbf{h}^2(x - x_{\mathbf{i}-1}) + 3\mathbf{h}(x - x_{\mathbf{i}-1})^2 - (x - x_{\mathbf{i}-1})^3 & x_{\mathbf{i}-1} \le x \le x_{\mathbf{i}} \\ \mathbf{h}^3 + 3\mathbf{h}^2(x_{\mathbf{i}+1} - x) + 3\mathbf{h}(x_{\mathbf{i}+1} - x)^2 - (x_{\mathbf{i}+1} - x)^3 & x_{\mathbf{i}} \le x \le x_{\mathbf{i}+1} \\ (x_{\mathbf{i}+2} - x)^3 & x_{\mathbf{i}+1} \le x \le x_{\mathbf{i}+2} \\ 0 & \text{otherwise} \end{cases} \tag{20}$$

and $\varrho_{\mathbf{i}}(t)$, $\upsilon_{\mathbf{i}}(t)$ are time dependent unknown quantities determined from the boundary conditions.

Using eqs. (19) and (20), we obtain the numerical solutions $\tilde{\Phi}(x, t)$ and $\tilde{\Psi}(x, t)$ of the BZ eq. (1) and it's derivatives up to second order in terms of $\varrho_i(t)$ and $\upsilon_i(t)$, respectively:

$$\tilde{\Phi}(x_{\mathbf{i}},t)=\varrho_{\mathbf{i}-1}(t)+4\varrho_{\mathbf{i}}(t)+\varrho_{\mathbf{i}+1}(t),\quad \tilde{\Phi}'_{\mathbf{i}}=\frac{-3}{\mathbf{h}}\left(\varrho_{\mathbf{i}-1}(t)-\varrho_{\mathbf{i}+1}(t)\right)$$
$$\tilde{\Phi}''_{\mathbf{i}}=\frac{6}{\mathbf{h}^2}\left(\varrho_{\mathbf{i}-1}(t)-2\varrho_{\mathbf{i}}(t)+\varrho_{\mathbf{i}+1}(t)\right) \tag{21}$$

$$\tilde{\Psi}(x_{\mathbf{i}},t)=\upsilon_{\mathbf{i}-1}(t)+4\upsilon_{\mathbf{i}}(t)+\upsilon_{\mathbf{i}+1}(t),\quad \tilde{\Psi}'_{\mathbf{i}}=\frac{-3}{\mathbf{h}}\left(\upsilon_{\mathbf{i}-1}(t)-\upsilon_{\mathbf{i}+1}(t)\right)$$
$$\tilde{\Psi}''_{\mathbf{i}}=\frac{6}{\mathbf{h}^2}\left(\upsilon_{\mathbf{i}-1}(t)-2\upsilon_{\mathbf{i}}(t)+\upsilon_{\mathbf{i}+1}(t)\right) \tag{22}$$

– *Procedure 4.* Substituting from eqs. (19), (21), and (22) into eq. (1), we obtain a general form equation is reached for the linearization technique:

$$\dot{\varrho}_{\mathbf{i}-1}(t)+4\dot{\varrho}_{\mathbf{i}}(t)+\dot{\varrho}_{\mathbf{i}+1}(t)-\frac{6}{\mathbf{h}^2}\left(\varrho_{\mathbf{i}-1}(t)-2\varrho_{\mathbf{i}}(t)+\varrho_{\mathbf{i}+1}(t)\right)-\left(\varrho_{\mathbf{i}-1}(t)+4\varrho_{\mathbf{i}}(t)+\varrho_{\mathbf{i}+1}(t)\right)+$$
$$+r\left(\varrho_{\mathbf{i}-1}(t)+4\varrho_{\mathbf{i}}(t)+\varrho_{\mathbf{i}+1}(t)\right)+\mathbf{Z}_{\mathbf{i}1}-r\mathbf{Z}_{\mathbf{i}2}=0$$
$$\dot{\upsilon}_{\mathbf{i}-1}(t)+4\dot{\upsilon}_{\mathbf{i}}(t)+\dot{\upsilon}_{\mathbf{i}+1}(t)-\frac{6}{\mathbf{h}^2}\left(\upsilon_{\mathbf{i}-1}(t)-2\upsilon_{\mathbf{i}}(t)+\upsilon_{\mathbf{i}+1}(t)\right)-b(\varrho_{\mathbf{i}-1}(t)+4\varrho_{\mathbf{i}}(t)+\varrho_{\mathbf{i}+1}(t))+$$
$$+b\mathbf{Z}_{\mathbf{i}2}=0 \tag{23}$$

where

$$\dot{\varrho}_{\mathbf{i}}(t)=\frac{\mathrm{d}\varrho}{\mathrm{d}t},\ \dot{\upsilon}_{\mathbf{i}}(t)=\frac{\mathrm{d}\upsilon}{\mathrm{d}t}$$
$$\mathbf{Z}_{\mathbf{i}1}=\Phi^2=\left(\varrho_{\mathbf{i}-1}(t)+4\varrho_{\mathbf{i}}(t)+\varrho_{\mathbf{i}+1}(t)\right)^2$$
$$\mathbf{Z}_{\mathbf{i}2}=\Phi\Psi=\left(\varrho_{\mathbf{i}-1}(t)+4\varrho_{\mathbf{i}}(t)+\varrho_{\mathbf{i}+1}(t)\right)\left(\upsilon_{\mathbf{i}-1}(t)+4\upsilon_{\mathbf{i}}(t)+\upsilon_{\mathbf{i}+1}(t)\right)$$

we described $\varrho_i(t)$, $\upsilon_i(t)$ and its derivatives with respect to time $\dot{\varrho}_i(t)$, $\dot{\upsilon}_i(t)$ with the finite difference scheme:

$$\varrho_{\mathbf{i}}(t)=\varrho_{\mathbf{i}}^{\mathbf{j}},\ \upsilon_{\mathbf{i}}(t)=\upsilon_{\mathbf{i}}^{\mathbf{j}},\ \ \dot{\varrho}_{\mathbf{i}}(t)=\frac{\varrho_{\mathbf{i}}^{\mathbf{j}+1}-\varrho_{\mathbf{i}}^{\mathbf{j}-1}}{2\Delta t},\ \dot{\upsilon}_{\mathbf{i}}(t)=\frac{\upsilon_{\mathbf{i}}^{\mathbf{j}+1}-\upsilon_{\mathbf{i}}^{\mathbf{j}-1}}{2\Delta t} \tag{24}$$

– *Procedure 5*. Replacing $\varrho_i(t)$, $\upsilon_i(t)$ and its first time derivatives in eq. (23) with eq. (24) and eliminating four unknowns ϱ_{-1}, $\varrho_{\mathbf{n}+1}$, υ_{-1}, $\upsilon_{\mathbf{n}+1}$, we get a system $(2\mathbf{n}+2)\times(2\mathbf{n}+2)$ of non-linear algebraic equations:

$$\mathbf{h}^2\varrho_{\mathbf{i}-1}^{\mathbf{j}+1}+4\mathbf{h}^2\varrho_{\mathbf{i}}^{\mathbf{j}+1}+\mathbf{h}^2\varrho_{\mathbf{i}+1}^{\mathbf{j}+1}+\left(-12\Delta t-2\Delta t\mathbf{h}^2+2\Delta t\mathbf{h}^2r\right)\varrho_{\mathbf{i}-1}^{\mathbf{j}}+\left(24\Delta t-8\Delta t\mathbf{h}^2+8\Delta t\mathbf{h}^2r\right)\varrho_{\mathbf{i}}^{\mathbf{j}}+$$
$$+\left(-12\Delta t-2\Delta t\mathbf{h}^2+2\Delta t\mathbf{h}^2r\right)\varrho_{\mathbf{i}+1}^{\mathbf{j}}-\mathbf{h}^2\varrho_{\mathbf{i}-1}^{\mathbf{j}-1}-4\mathbf{h}^2\varrho_{\mathbf{i}}^{\mathbf{j}-1}-\mathbf{h}^2\varrho_{\mathbf{i}+1}^{\mathbf{j}-1}+2\Delta t\mathbf{h}^2\mathbf{Z}_{\mathbf{i}1}-2\Delta t\mathbf{h}^2r\mathbf{Z}_{\mathbf{i}2}=0$$
$$\mathbf{h}^2\upsilon_{\mathbf{i}-1}^{\mathbf{j}+1}+4\mathbf{h}^2\upsilon_{\mathbf{i}}^{\mathbf{j}+1}+\mathbf{h}^2\upsilon_{\mathbf{i}+1}^{\mathbf{j}+1}-12\Delta t\upsilon_{\mathbf{i}-1}^{\mathbf{j}}+24\Delta t\upsilon_{\mathbf{i}}^{\mathbf{j}}-12\Delta t\upsilon_{\mathbf{i}+1}^{\mathbf{j}}-\mathbf{h}^2\upsilon_{\mathbf{i}-1}^{\mathbf{j}-1}-4\mathbf{h}^2\upsilon_{\mathbf{i}}^{\mathbf{j}-1}-\mathbf{h}^2\upsilon_{\mathbf{i}+1}^{\mathbf{j}-1}-$$
$$-2b\Delta t\mathbf{h}^2\varrho_{\mathbf{i}-1}^{\mathbf{j}}-8b\Delta t\mathbf{h}^2\varrho_{\mathbf{i}}^{\mathbf{j}}-2b\Delta t\mathbf{h}^2\varrho_{\mathbf{i}+1}^{\mathbf{j}}+2b\Delta t\mathbf{h}^2\mathbf{Z}_{\mathbf{i}2}=0 \tag{25}$$

can be evaluated by Mathematica program.

– *Procedure 6.* To show the presented numerical method is highly efficient and effective, we compute the L_2 and L_1 norms:

$$L_2 = \sqrt{\mathbf{h}\sum_{\mathbf{i}=0}^{\mathbf{n}}(\Phi_{\mathbf{i}}^{\mathbf{j}} - \tilde{\Phi}_{\mathbf{i}}^{\mathbf{j}})^2} = \sqrt{\mathbf{h}\sum_{\mathbf{i}=0}^{\mathbf{n}}(\Psi_{\mathbf{i}}^{\mathbf{j}} - \tilde{\Psi}_{\mathbf{i}}^{\mathbf{j}})^2}, \quad L_\infty = \max_{\mathbf{i}=0}^{\mathbf{n}}\left|\Phi_{\mathbf{i}}^{\mathbf{j}} - \tilde{\Phi}_{\mathbf{i}}^{\mathbf{j}}\right| = \max_{\mathbf{i}=0}^{\mathbf{n}}\left|\Psi_{\mathbf{i}}^{\mathbf{j}} - \tilde{\Psi}_{\mathbf{i}}^{\mathbf{j}}\right| \tag{26}$$

We discuss at length our obtained numerical results corresponding to the analytical solutions eqs. (15) and (16) for bromous acid concentration (Φ) and bromide ion concentration (Ψ) that introduced in the BZ reaction-diffusion model.

We present the errors L_2 and L_∞ correspond to Φ and Ψ for different step lengths **h** and different times, t, with time level $\Delta t = 0.01$ using the parameters eq. (13) at $r = 0.3$, $\mu = 0.0001$, $\lambda = 0.4$, $h_1 = 0.8$, and $h_2 = 0.1$ for the analytical solution eq. (15) and $r = 1.01$, $\mu = 0.001$, $\lambda = 0.01$, $h_1 = 0.5$, and $h_2 = 0.1$ for the analytical solution eq. (16) as in tabs. 1 and 2, respectively. The results show L_∞ error norm is smaller than L_2 error norm. Thus, we can observe the proposed numerical method is satisfactorily accurate. Figures 4 and 6 show the numerical solutions and the analytical solutions of the BZ reaction-diffusion model at time $t = 10$. Figures 5 and 7 exhibit the maximum absolute errors for the analytical solution eqs. (15) and (16) with parameters eq. (13), respectively. While, fig. 8 display the analytical and numerical solutions of the BZ reaction-diffusion model at level $t = 10$ using different value of the parameter b.

Table 1. The L_2 and L_∞ norms with time level $\Delta t = 0.01$ and different step lengths h and values for the BZ equation using eq. (15) and parameters eq. (13)

t	**h** = 1.0				**h** = 2.0			
	Φ(x, t)		Ψ(x, t)		Φ(x, t)		Ψ(x, t)	
	L_∞	L_2	L_∞	L_2	L_∞	L_2	L_∞	L_2
0.2	$3.2873 \cdot 10^{-5}$	$5.8010 \cdot 10^{-5}$	$3.1513 \cdot 10^{-4}$	$6.6156 \cdot 10^{-4}$	$1.0292 \cdot 10^{-4}$	$3.3109 \cdot 10^{-4}$	$1.2589 \cdot 10^{-3}$	$3.7984 \cdot 10^{-3}$
0.4	$6.2998 \cdot 10^{-5}$	$1.1151 \cdot 10^{-4}$	$5.6152 \cdot 10^{-4}$	$1.2338 \cdot 10^{-3}$	$1.8900 \cdot 10^{-4}$	$6.3309 \cdot 10^{-4}$	$2.2106 \cdot 10^{-3}$	$7.0603 \cdot 10^{-3}$
0.6	$8.7217 \cdot 10^{-5}$	$1.6022 \cdot 10^{-4}$	$7.9480 \cdot 10^{-4}$	$1.7433 \cdot 10^{-3}$	$3.0371 \cdot 10^{-4}$	$9.0561 \cdot 10^{-4}$	$2.8822 \cdot 10^{-2}$	$9.9504 \cdot 10^{-3}$
0.8	$1.0631 \cdot 10^{-4}$	$2.0404 \cdot 10^{-4}$	$1.0141 \cdot 10^{-4}$	$2.2166 \cdot 10^{-3}$	$4.1368 \cdot 10^{-4}$	$1.1489 \cdot 10^{-3}$	$3.4677 \cdot 10^{-3}$	$1.2616 \cdot 10^{-2}$
0.0	$1.3293 \cdot 10^{-4}$	$2.4502 \cdot 10^{-4}$	$1.2037 \cdot 10^{-4}$	$2.9300 \cdot 10^{-3}$	$5.0646 \cdot 10^{-4}$	$1.3641 \cdot 10^{-3}$	$4.5675 \cdot 10^{-3}$	$1.5181 \cdot 10^{-2}$

Table 2. The L_2 and L_∞ norms with time level $\Delta t = 0.01$ and different step lengths h and values for the BZ equation using eq. (16) and parameters eq. (13)

t	**h** = 1.0				**h** = 2.0			
	Φ(x, t)		Ψ(x, t)		Φ(x, t)		Ψ(x, t)	
	L_∞	L_2	L_∞	L_2	L_∞	L_2	L_∞	L_2
0.2	$7.5488 \cdot 10^{-10}$	$2.2582 \cdot 10^{-9}$	$1.3613 \cdot 10^{-8}$	$3.5239 \cdot 10^{-8}$	$9.2030 \cdot 10^{-9}$	$3.0076 \cdot 10^{-8}$	$1.1955 \cdot 10^{-7}$	$3.7153 \cdot 10^{-7}$
0.4	$1.5543 \cdot 10^{-10}$	$4.4989 \cdot 10^{-9}$	$2.7970 \cdot 10^{-8}$	$7.2512 \cdot 10^{-8}$	$1.7493 \cdot 10^{-8}$	$5.8102 \cdot 10^{-8}$	$2.2430 \cdot 10^{-7}$	$7.0264 \cdot 10^{-7}$
0.6	$2.5555 \cdot 10^{-9}$	$6.7824 \cdot 10^{-9}$	$4.5458 \cdot 10^{-8}$	$1.1281 \cdot 10^{-7}$	$2.4993 \cdot 10^{-8}$	$8.4305 \cdot 10^{-8}$	$3.1598 \cdot 10^{-7}$	$9.9669 \cdot 10^{-7}$
0.8	$5.7484 \cdot 10^{-9}$	$1.1041 \cdot 10^{-8}$	$6.7325 \cdot 10^{-8}$	$1.8068 \cdot 10^{-7}$	$3.1803 \cdot 10^{-8}$	$1.0889 \cdot 10^{-7}$	$3.9602 \cdot 10^{-7}$	$1.2566 \cdot 10^{-6}$
0.0	$2.6101 \cdot 10^{-8}$	$4.9115 \cdot 10^{-8}$	$3.6737 \cdot 10^{-7}$	$7.0858 \cdot 10^{-7}$	$3.8010 \cdot 10^{-8}$	$1.3203 \cdot 10^{-7}$	$4.6565 \cdot 10^{-7}$	$1.4854 \cdot 10^{-6}$

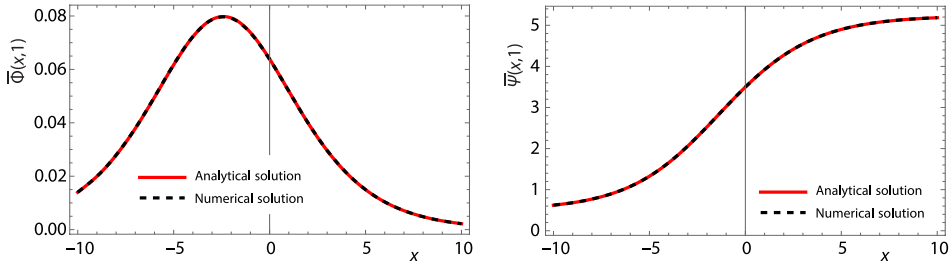

Figure 4. Numerical and analytical results of the BZ equation using eq. (15) with parameters eq. (13) at $r = 0.3$, $\mu = 0.0001$, $\lambda = 0.4$, $h_1 = 0.8$, and $h_2 = 0.1$, time $t = 1.0$ with $\Delta t = 0.1$ and h = 1.0

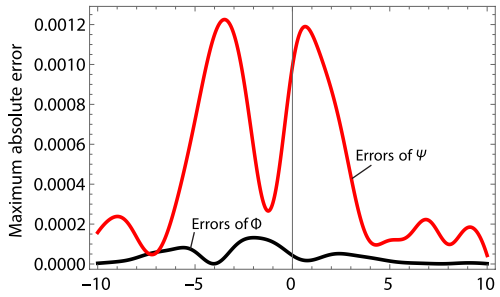

Figure 5. Maximum absolute errors of the BZ equation using eq. (15) with parameters eq. (13) at $r = 0.3$, $\mu = 0.0001$, $\lambda = 0.4$, $h_1 = 0.8$, and $h_2 = 0.1$, time $t = 1.0$ with $\Delta t = 0.001$ and h = 1.0

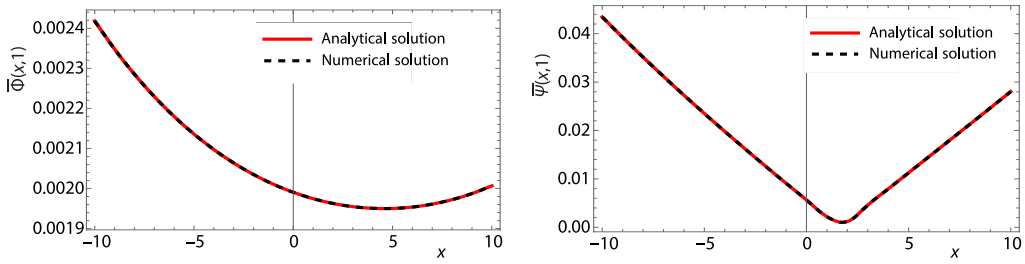

Figure 6. Numerical and analytical results of the BZ equation using eq. (16) with parameters eq. (13) at $r = 1.01$, $\mu = 0.001$, $\lambda = 0.01$, $h_1 = 0.5$, and $h_2 = 0.1$, time $t = 1.0$ with $\Delta t = 0.1$ and h = 1.0

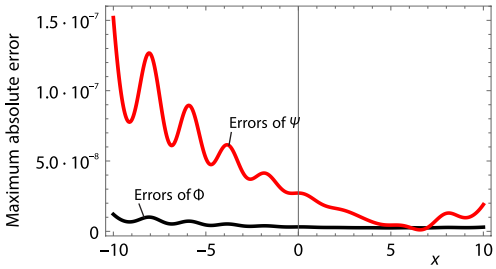

Figure 7. Maximum absolute errors of the BZ equation using eq. (16) with parameters eq. (13) at $r = 1.01$, $\mu = 0.001$, $\lambda = 0.01$, $h_1 = 0.5$, and $h_2 = 0.1$, time $t = 1.0$ with $\Delta t = 0.001$ and h = 1.0

Conclusion

Our research indicates that the system of equations examined serves as an effective model for comprehending the dynamics of complex non-linear systems. This system demonstrated a variety of intriguing behaviors, such as oscillations and spatial patterns. Notably, vari-

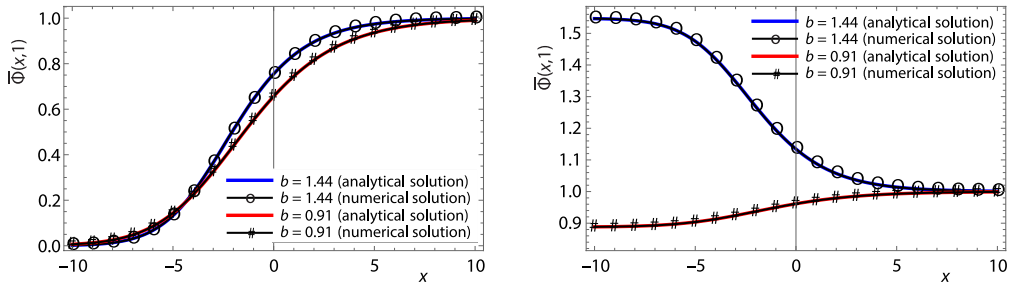

Figure 8. Analytical and numerical results of the BZ equation using eq. (15) and Set 2 eq. (14) at level t = 1.0 with Δt = 0.1 and h = 0.1, (r = 0.8,μ = 0.001, λ = 0.3, h_1 = 0.3, and h_2 = 0.1, and b = 1.44, b = 0.91

ations in the parameter b can profoundly influence the system's dynamics, resulting in diverse oscillatory behaviors, including periodic, quasi-periodic, and chaotic patterns. Understanding how these parameters affect the system is crucial for predicting its behavior and for designing experiments related to the BZ reaction. The exact solutions derived using the (G'/G)-expansion technique offer valuable insights into these dynamics and could guide future research in this field. We anticipate that the solutions obtained will be instrumental in testing various models that simulate the behavior of the BZ chemical reaction, enhancing our understanding of its mechanisms. Our results include hyperbolic, trigonometric, and rational solutions, showcasing a range of optical solitons, such as periodic, dark, and bright solitons. Moreover, we implemented a numerical scheme based on the cubic B-spline method for the BZ reaction-diffusion model, as outlined in eq. (1). The accuracy and efficiency of this numerical approach are illustrated in tabs. 1 and 2, as well as fig. 4 through fig. 8. The effectiveness and potential of the techniques employed are evident in the results obtained.

Acknowledgment

The authors extend their appreciation Taif University, Saudi Arabia, for supporting this work through Project No. (TU-DSPP-2024-73).

References

[1] Murray, J. D., *Non-Linear Differential Equations in Biology*, Lectures on Models Russian translation, Mir, Moscow, Russia, 1983
[2] Murray, J. D., *Mathematical Biology II: Spatial Models and Biomedical Applications*, 3rd ed., Springer, New York, USA, 2002
[3] Lin, G., *et al*., Travelling Wavefronts of Belousov-Zhabotinskii System with Diffusion and Delay, *Applied Mathematics Letters*, *22* (2009), 3, pp. 341-346
[4] Murray, J. D., *Mathematical Biology*, Springer, New York, USA, 1989
[5] Murray, J. D., On Traveling Wave Solutions in A Model for B-Z Reaction, *J. Theor. Biol*., *56* (2009), 2, pp. 329-353
[6] Tyson, J. J., *The Belousov-Zhabotinskii Reaction, Lecture Notes in Biomathematics*, Springer, New York, USA, Vol. 10, 1976
[7] Ye, Q. X., *et al*., Travelling Wave Front Solutions of Noyes-Field System for Belousov-Zhabotinskii Reaction, *Non-Linear Analysis TMA*, *11* (1987), 11, pp. 1289-1302
[8] Ye, Q., Wang, M., A Note on Travelling Wave Solutions for Belousov-Zhabotinskii Chemical Reaction, *Transactions of Beijing Inst. of Technol.*, (1989), 4, pp. 5-9
[9] Li, Z. Y., The Existence of Travelling Front Solutions for Reaction-Diffusion System, *J. Partial Differential Equations*, *5* (1992), Aug., pp. 17-22
[10] Li, Z., Ye, Q., Travelling Wave Front Solutions for Reaction-Diffusion Systems, *J. Partial Differential Equations*, *4* (1991), 3, pp. 1-14

[11] Trofimchuk, E., *et al*., Traveling Waves for a Model of the Belousov-Zhabotinsky Reaction, *Journal of Differential Equations*, *254* (2013), 9, pp. 3690-3714
[12] Manoranjan, V. S., *et al*., A Numerical Study of the Belousov-Zhabotinskii Chemical Reaction Using Galerkin Finite Element Method, *J. Math. Biol*, *16* (1983), Feb., pp. 251-260
[13] Wang, M., *et al.*, Explicit Wave Front Solutions of Noyes-Field Systems for the Belousov-Zhabotinskii Reaction, *Journal of Mathematical Analysis and Applications*, *182* (1994), 3, pp. 705-717
[14] Quinney, D. A., On Computing Travelling Wave Solutions in a Model for the Belousov Zhabotinskii Reaction, *J. Inst. Maths Applies*, *23* (1979), 2, pp. 193-201
[15] Kudryashov, N. A., *et al*., Painleve Analysis and Exact Solutions for the Belousov-Zhabotinskii Reaction-Diffusion System, *Chaos, Solitons and Fractals*, *65* (2014), Aug., pp. 111-117
[16] Prenter, P. M., *Splines and Variational Methods*, John Wiley and Sons, New York, USA, 1975
[17] Karakoc, S. B. G., *et al*., A cubic B Spline Galerkin Approach for the Numerical Simulation of the GEW Equation, Statistics, *Optimization and Information Computing*, *4* (2016), 1, pp. 30-41
[18] Karakoc, S. B. G., A New Numerical Application of the Generalized Rosenau-RLW Equation, Scientia *Iranica B, 27* (2020), 2, pp. 772-783
[19] Karakoc, S. B. G., *et al.*, A Numerical Investigation of the GRLW Equation Using Lumped Galerkin Approach with Cubic B Spline, *Springer Plus*, *5* (2016), 199, pp. 1-17
[20] Hadhoud, A. R., *et al.*, A Septic B-Spline Collocation Method for Solving Non-Linear Singular Boundary Value Problems Arising in Physiological Models, *Scientia Iranica E*, *27* (2020), 3, pp. 1674-1684
[21] Geyikli, T., *et al*., Subdomain Finite Element Method with Quartic B Splines for the Modified Eqaul Width Wave Equation, *Computational Mathematics and Mathematical Physics*, *55* (2015), 3, pp. 410-421
[22] Raslan, K. R., *et al*., Numerical Study of MHD-Duct Flow Using the 2-D Finite Difference Method, *Appl. Math. Inf. Sci*., *14* (2020), 4, pp. 1-5
[23] EL-Danaf, T. S., *et al.*, New Numerical Treatment for the Generalized Regularized Long Wave Equation Based on Finite Difference Scheme, *Int. J. of S. Comp. and Eng*., *4* (2014), 4, pp. 16-24
[24] Raslan, K. R., *et al*., Bi-Finite Difference Method to Solve Second-Order Non-Linear Hyperbolic Telegraph Equation in Two Dimensions, *Mathematical Problems in Engineering*, *2022* (2022), 1782229
[25] Durur, H., Different Types Analytic Solutions of the (1+1)-Dimensional Resonant Non-Linear Schrodinger's Equation Using G'/G-expansion Method, *Modern Physics Letters B*, *34* (2020), 2, 2050036
[26] Wang, M., *et al*., G'/G-Expansion Method And Travelling Wave Solutions Of Non-Linear Evolution Equations in Mathematical Physics, *Physics Letters A*, *372* (2008), 4, pp. 417-423
[27] Almusawa, H., *et al.*, Protracted Study on a Real Physical Phenomenon Generated by Media Inhomogeneities, *Results in Physics*, *31* (2021), 104933

Paper submitted: May 19, 2024
Paper revised: September 20, 2024
Paper accepted: October 17, 2024